Mott transition in the Hubbard model away from particle-hole symmetry

D. J. García,[1] E. Miranda,[1] K. Hallberg,[2] and M. J. Rozenberg[3,4]

[1]*Instituto de Física Gleb Wataghin, Unicamp, CEP 13083-970 Campinas, SP, Brazil*
[2]*Instituto Balseiro and Centro Atómico Bariloche, CNEA, (8400) San Carlos de Bariloche, Argentina*
[3]*Laboratoire de Physique des Solides, CNRS-UMR8502, Université de Paris-Sud, Orsay 91405, France*
[4]*Departamento de Física, FCEN, Universidad de Buenos Aires, Ciudad Universitaria, Pabellón 1, Buenos Aires (1428), Argentina*

We solve the dynamical mean-field theory equations for the Hubbard model away from the particle-hole-symmetric case using the density matrix renormalization group method. We focus our study on the region of strong interactions and finite doping where two solutions coexist. We obtain precise predictions for the boundaries of the coexistence region. In addition, we demonstrate the capabilities of this precise method by obtaining the frequency-dependent optical conductivity spectra.

PACS number(s): 71.10.Fd, 71.27.+a, 71.30.+h

Introduction. Solving models for strongly correlated compounds (typically those including d or f electrons) remains a hard and important open problem of modern condensed matter physics. In these systems interesting anomalous behavior usually occurs as a consequence of the competition between the kinetic and Coulomb energies of electrons, which are of the same order of magnitude, and analytical methods based on perturbative considerations are notoriously unreliable. Therefore, one is led to resort to nonperturbative techniques and numerical methods to try to deal with these difficulties.

In recent years, a nonperturbative approach to general strongly correlated electron models, termed dynamical mean-field theory (DMFT),[1,2] allowed progress in the understanding of several physical problems, including the correlation-driven Mott metal-insulator transition. The key feature of DMFT is that it maps the original lattice problem onto a self-consistent quantum impurity model. This resulting quantum impurity remains, nevertheless, a fully interacting many-body problem that has to be solved.[1] The success of DMFT in dealing with model Hamiltonians has generated a great deal of interest in combining it with *ab initio* band structure methods with the goal of obtaining a realistic description of correlated electron compounds.[2] The main technical difficulty is the lack of a reliable method to solve the associated quantum impurity problem. Currently, the most widely adopted methodology is the quantum Monte Carlo technique, which generally requires an analytical continuation of the results to the real frequency axis. Unfortunately, the latter introduces some uncertainty in the procedure, which becomes a severe problem for multiorbital systems. Therefore, there is strong interest in the development of new methods that can deal with general quantum impurity models directly on the real axis. An interesting proposal was recently introduced which was based on the precise diagonalization of the quantum impurity Hamiltonian with the powerful density matrix renormalization group (DMRG) method.[3–5] This technique has the virtue of being already widely employed in the study of low-dimensional strongly correlated systems and is based on a judicious trimming of the Hilbert space so as to restrict the numerical calculation to its most relevant subspace.[6] In this manner, despite the exponential growth of the Hilbert space, hundreds of orbitals can be taken into account. Moreover, the method is not restricted to the ground

state and finite energy excitations can be computed with similar accuracy.[7] This is in contrast to the related alternative, the numerical renormalization group (NRG) method, which aims at a very precise description of the low-frequency quasiparticle peaks associated with low-energy excitations, as done in its celebrated application to the Kondo problem.[8] The DMRG method, on the other hand, treats high and low frequencies on an equal footing.

The initial DMRG solution of the DMFT equations was obtained for the simplest test case of the particle-hole symmetric Hubbard model.[3–5] In this Rapid Communication we show that the method can reliably tackle the general finite doping case. In particular we focus on the most demanding region of the phase diagram where two solutions coexist near the correlation-driven Mott metal-insulator transition and obtain the phase boundaries with unprecedented precision. We also illustrate the capabilities of the methodology by computing the frequency-dependent optical conductivity, which requires a reliable description of higher-energy features, such as the Hubbard bands, that lie beyond the scope of the NRG method. Our results show that even at the smallest dopings and strong interaction strength, the low-frequency contribution to the optical conductivity, the Drude part, remains very well described by a Lorentzian line shape. We also show that both the vanishing of the Drude weight or the doping can signal equally well the destruction of the correlated Fermi liquid metallic state. Our work amounts to a substantial improvement with respect to previous studies based on exact diagonalization [of up to eight sites; however, nowadays somewhat larger systems are possible with exact diagonalization (ED)] and an *ad hoc* perturbation scheme,[9] and opens the way for the application of the DMFT+DMRG method to more general model Hamiltonians. Details of the method will be given elsewhere.[10]

The Model. The Hamiltonian of the Hubbard model is defined by

$$H = \frac{t}{\sqrt{2d}} \sum_{\langle i,j \rangle, \sigma} c_{i,\sigma}^{\dagger} c_{j,\sigma} + U \sum_i \left(n_{i,\uparrow} - \frac{1}{2} \right) \left(n_{i,\downarrow} - \frac{1}{2} \right) - \mu \sum_{i,\sigma} n_{i,\sigma}, \quad (1)$$

where U is the on-site Coulomb interaction, μ is the chemical potential, t is the hopping, and d is the space dimension.
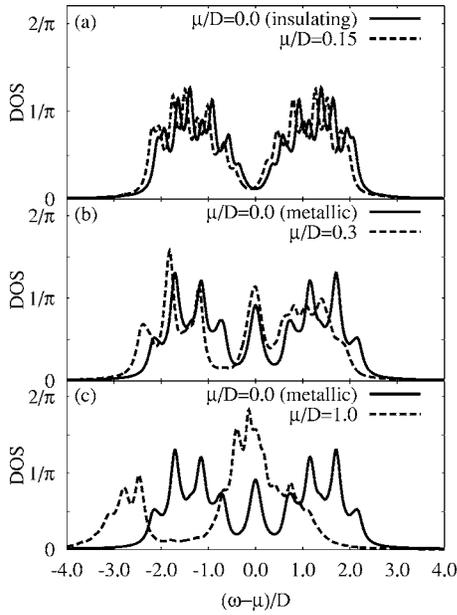
FIG. 1. (a) Insulating, (b) lightly doped, and (c) heavily doped metallic densities of states (DOS) of the Hubbard model for U/D =2.6. In (a), the small DOS weight seen at $\omega=0$ is due to the relatively large relation between the gap for U/D=2.6 ($\sim$0.19) and the small Lorentzian broadening used (η=0.1).

We take the half bandwidth of the noninteracting model as the unit of energy; thus, $D=2t=1$. We particularize to the case of the infinite-dimensional Bethe lattice, in which the noninteracting density of states (DOS) is $D(\epsilon)=(2/\pi)\sqrt{1-\epsilon^2}$.

The associated impurity problem is the single-impurity Anderson model (SIAM), and its hybridization function needs to be self-consistently determined.[1] The SIAM Hamiltonian is solved in linear chains[11,12] using the DMRG algorithm[3] of up to 101 sites, keeping 128 states per block.

We focus our study on the poorly explored region of the U-μ parameter space where two solutions, insulating and metallic, can be obtained from the DMFT equations. In Fig. 1 we show the evolution of the DOS for the two solutions as one moves away from the half-filled particle-hole-symmetric case. The chemical potential μ is increased at fixed U. While the use of the DMRG method allows the precise diagonalization of the associated SIAM problem with a bath that can be accurately described using around 100 sites, this impurity model remains, nevertheless, finite. Therefore, the computed Green's functions contain a finite, though large, number of poles. Thus, as in any exact diagonalization scheme, one needs to broaden the poles to allow the observation of the DOS structure on the real axis.

Results. We show in Fig. 1 the results obtained by using a simple Lorentzian broadening η. We find that choice to be more appropriate than the "logarithmic" broadening usually adopted in NRG calculations[13,14] which, although capable of sharply resolving the insulating gap, tends to wash out the high-energy features of the density of states. The results show that, in the insulating case, when the chemical potential is moved within the Mott gap, the lower and upper Hubbard bands shift rigidly, without any ostensible transfer of spectral

weight taking place [Fig. 1(a)]. The apparent substructure in the Hubbard bands seen in the insulating DOS results from finite-size effects,[15]—i.e., a finite number of poles. Our finite-size analysis (not shown) suggests that in the infinite-chain limit the Hubbard bands become smooth. This is in contrast to what is seen in the large-U/D antiferromagnetic phase.[16] In the lightly doped case one observes that, as the central quasiparticle peak rapidly moves through the region between the Hubbard bands, there is a transfer of spectral weight as well as an evolution of the line shapes [Fig. 1(b)]. More precisely, one finds that the quasiparticle peak receives spectral weight from both Hubbard bands. For larger values of μ, as the system gets heavily doped, one finds that the quasiparticle peak eventually broadens as it merges with the closest Hubbard band [Fig. 1(c)]. As these features coalesce, they also draw spectral weight from the other Hubbard band, which remains at an energy distance of the order of U.[1]

In order to demonstrate the capabilities of the method we shall now compute the frequency-dependent optical conductivity. From the lattice Green's $G(\epsilon_k, \nu)$ function, where ϵ_k is the noninteracting dispersion, we can evaluate the optical conductivity within DMFT as[1,17]

$$\text{Re } \sigma(\omega + I0^+) = \frac{\pi e^2}{\hbar a d} \int_\infty^\infty d\epsilon D(\epsilon) \int_\infty^\infty d\nu \rho(\epsilon, \nu) \rho(\epsilon, \nu + \omega)$$

$$\times \frac{\theta(\nu + \omega) - \theta(\nu)}{\omega}, \qquad (2)$$

where a is the lattice spacing, d is the spatial dimension, $\rho(\epsilon, \nu) = \text{Im } G(\epsilon, \nu - I0^+)/\pi$, and $I0^+$ denotes an infinitesimal imaginary part. For simplicity we have chosen to use a unitary vertex. The evaluation of $\rho(\epsilon, \nu)$ requires a previous computation of the local self-energy. While in the standard exact diagonalization solution of the DMFT equations this is a cumbersome procedure due to the small number of Green's function poles, the use of the DMRG method dramatically changes the situation and reliable $\Sigma(\omega)$ on the real axis can be easily obtained from the self-consistency condition.[1] In Fig. 2 we show the optical conductivity for two coexistent solutions (for parameters U/D=2.6 and μ=0.2) and for the metallic state for weak interaction (U/D=0.6). In the metallic case we see that, despite the very small doping, the small frequency regime of $\sigma(\omega)$ can be very well described by a simple Lorentzian form that follows from a Drude model[18]

$$\text{Re } \sigma(\omega + I0^+) = \frac{\text{DW} \times \tau}{1 + (\omega\tau)^2}, \qquad (3)$$

where τ is the relaxation time and DW is the Drude weight, which is a measure of the number of quasiparticle carriers in the metal.[19] In our metallic case the finite value of τ^{-1} comes from the finite imaginary part used to compute the Green's function G. The inset shows that as η goes to zero, τ^{-1} tends to zero and we recover the δ-function behavior that corresponds to a clean Fermi liquid. For large U/D we observe that, in addition to the small Drude part, the optical conductivity spectrum has a large midinfrared contribution at frequencies of order U. This regular part corresponds to finite-frequency optical excitations between the two Hubbard
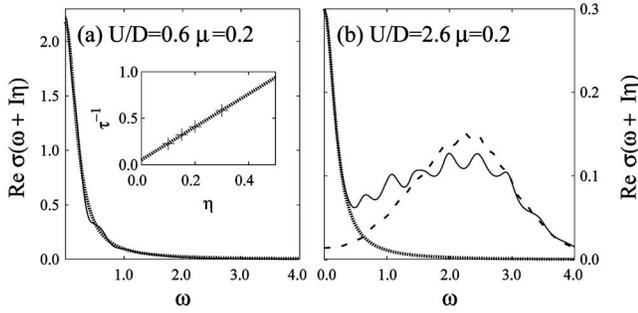
FIG. 2. Metallic (solid line) and insulating (dashed line) optical conductivities for the Hubbard model in the purely metallic (a) and coexistent (b) regimes. The dotted line is a Lorentzian low-frequency fit (Drude model). For small U/D, the data and the Lorentzian fit agree in almost all the frequency range. The broad feature in (b) corresponds to the regular part explained in the text. A small imaginary part $\eta=0.1$ has been used. The inset shows the evolution of τ in the Lorentzian fit of the low-frequency conductivity as a function of η for $U/D=0.6$.

bands and between the latter and the central quasiparticle peak and is almost absent for small values of the Coulomb interaction.

The destruction of a normal metallic state is formally defined by the vanishing of the Drude weight, which signals the localization of all metallic conduction carriers.[20] On the other hand, in the Hubbard model it is well known that, unless in phases with some type of long-range order or in the presence of disorder, infinitesimal doping at $T=0$ is enough to drive the system across a density driven metal-insulator transition. Therefore, a demanding test for the present method would be to verify that both the doping $\delta=(n-1)/2$ (where n is the number of particles per site) and the Drude weight vanish at the same value of interaction strength. We emphasize the important technical fact that, while the value of the doping is simply and accurately computed from the expectation value of the number operator, the Drude weight is, in contrast, independently obtained via the comparatively far more laborious procedure described above. The comparison of the results of panels (a) and (b) of Fig. 3 shows that, in fact, both observables δ and DW are found to vanish at equal interaction values for each choice of the chemical potential.

Figure 3(a) shows the evolution of the doping for fixed chemical potential, varying the Coulomb interaction. The doping increases as μ moves to larger values—i.e., away from the particle-hole case. At fixed μ, increasing the correlation U from the noninteracting limit acts to decrease δ continuously to 0, where the metallic solution is no longer stable and gives rise to the insulating one. The extrapolation of the lowest doping values towards zero for different chemical potentials provides an accurate estimate of the critical line $\mu_{c2}(U)$ which locates the instability of the metal towards an insulating solution. The Drude weight is shown in Fig. 3(b). Its behavior is qualitatively different from that of δ, since DW(U) does not uniformly increase with increasing μ. In the low-U/D region, the DW decreases as the chemical potential is increased, reflecting the lowering of the kinetic energy due to the fewer number of carriers. In contrast, for
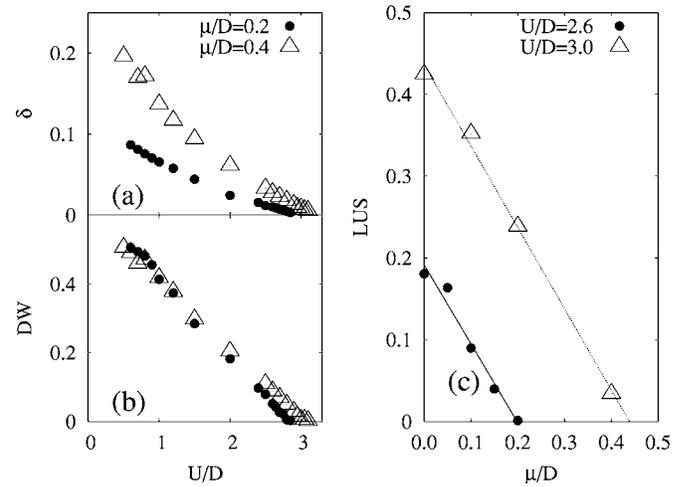
FIG. 3. (a) Doping δ and (b) Drude weight (DW) for the metallic states for various U/D and μ/D values. (c) Energy of the lowest unoccupied state (LUS) in the upper Hubbard band for insulating solutions.

larger values of the interaction close to the μ_{c2} line, the DW decreases as μ decreases towards particle-hole symmetry, reflecting the enhancement of the effective mass as the metal-insulator transition is approached.

It is also possible to investigate the instability of the insulating state towards the metal. This transition is signaled by the collapse of the Mott-Hubbard gap as the chemical potential is brought to a Hubbard band edge. Following the energy of the lowest unoccupied state (LUS) in the upper Hubbard band with respect to the Fermi level in the insulator as μ increases, it is possible to determine the transition line $\mu_{c1}(U)$ [Fig. 3(c)] as the value of the critical chemical potential for which the energy of the LUS vanishes. As the bands move in an approximately rigid way for $\mu < \mu_{c1}(U)$ the value of the chemical potential varies linearly and agrees with half the size of the band gap at $\mu=0$ (see Fig. 4). For $\mu > \mu_{c1}(U)$ a finite number of poles appears at positive and negative small values of $\omega-\mu$, signaling the metallic state.

The critical lines allow us to accurately draw the phase diagram of the model away from particle-hole symmetry at $T=0$. Previous work has been restricted to either a small number of sites[9] in the effective impurity Hamiltonian or to
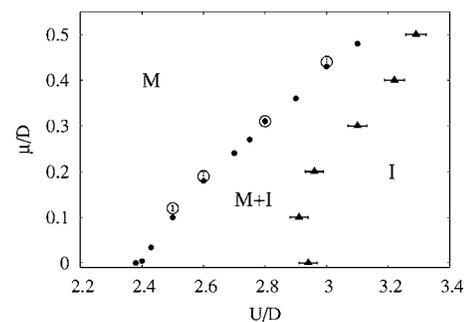
FIG. 4. Phase diagram: Small solid circles show half the gap value for $\mu=0$. Open circles (solid triangles) are the extrapolated critical values of the chemical potential μ_{c1} (μ_{c2}) where the insulating (metallic) solution no longer exists.

small but finite temperatures using quantum Monte Carlo simulations.[21] On the other hand, the NRG method is not very well suited for an accurate investigation of the insulating state. In Fig. 4 we plot the $\mu_{c1}(U)$ and $\mu_{c2}(U)$ lines that determine three regions in the μ-U phase diagram: For $\mu > \mu_{c1}(U)$ [$\mu < \mu_{c2}(U)$] only metallic [insulating] solutions are found. In the middle there is a region of coexistence of both kinds of states, where the metallic state is one with the lowest energy.[1] The phase diagram presented here shows an overall agreement with the one obtained through exact diagonalization in the "star geometry"[9] where the impurity site is connected with hopping terms to all the other sites. The main differences are found for the $\mu_{c2}(U)$ line because, as the metal-to-insulator transition is approached, the quasiparticles develop a diverging mass corresponding to a very narrow quasiparticle peak. In the language of the associated SIAM, this narrow resonance implies a large correlation length which can be fully realized only in long enough systems. This can only be obtained with the method presented here, allowing for very accurate results.

Conclusions. In this work we have shown that the DMRG method, in addition to being largely used to compute spectral quantities of low-dimensional strongly correlated systems,[7,6] allows for a practical implementation of an accurate impurity solver of the DMFT equations of the Hubbard model in a general case. We have computed spectral functions including the DOS and the frequency-dependent optical conductivity. We have also calculated the behavior of the doping and the Drude weight as a function of the chemical potential near the metal-insulator transition and demonstrated the accuracy of the method by passing the demanding test of the comparison of their respective predictions for the metal-insulator critical line. Due to the fact that with this method long enough systems can be handled, these critical lines can be very accurately obtained. Of course, in the nonfrustrated case the true ground state of the model is antiferromagnetic at low doping and the extension of the method to that case is left for future work.

The implementation of the DMRG method for the Hubbard model in the nonsymmetric case is an important step towards achieving an exact, unbiased, and general impurity solver to be used in the realistic *ab initio* strongly correlated electronic structure calculation program.[2] The next step ahead is to generalize the methodology for the multiorbital case, where interesting physical problems remain open, such as the orbital-selective Mott transition with a fully rotationally invariant Hamiltonian.

[1] A. Georges, G. Kotliar, W. Krauth, and M. J. Rozenberg, Rev. Mod. Phys. **68**, 13 (1996).

[2] G. Kotliar and D. Vollhardt, Phys. Today **57**(3), 53 (2004).

[3] D. J. García, K. Hallberg, and M. J. Rozenberg, Phys. Rev. Lett. **93**, 246403 (2004).

[4] S. Nishimoto, F. Gebhard, and E. Jeckelmann, J. Phys.: Condens. Matter **16**, 7063 (2004).

[5] M. Karski, C. Raas, and G. S. Uhrig, Phys. Rev. B **72**, 113110 (2005).

[6] *Density Matrix Renormalization*, edited by I. Peschel, X. Wang, M. Kaulke, and K. Hallberg, Lectures Notes in Physics (Springer-Verlag, Berlin, 1999); S. R. White, Phys. Rev. Lett. **69**, 2863 (1992); see also the recent reviews U. Schollwöck, Rev. Mod. Phys. **77**, 259 (2005); K. Hallberg, Adv. Phys. **55**, 477 (2006).

[7] K. A. Hallberg, Phys. Rev. B **52**, R9827 (1995); S. Ramasesha *et al.*, Synth. Met. **85**, 1019 (1997); T. D. Kühner and S. R. White, Phys. Rev. B **60**, 335 (1999); E. Jeckelmann, *ibid.* **66**, 045114 (2002).

[8] K. G. Wilson, Rev. Mod. Phys. **55**, 583 (1983).

[9] H. Kajueter and G. Kotliar, Phys. Rev. Lett. **77**, 131 (1996); H. Kajueter, G. Kotliar, and G. Moeller, Phys. Rev. B **53**, 16214 (1996).

[10] D. Garcia *et al.* (unpublished).

[11] Q. Si, M. J. Rozenberg, G. Kotliar, and A. E. Ruckenstein, Phys. Rev. Lett. **72**, 2761 (1994).

[12] M. J. Rozenberg, G. Moeller, and G. Kotliar, Mod. Phys. Lett. B **8**, 535 (1994).

[13] R. Bulla, Phys. Rev. Lett. **83**, 136 (1999).

[14] R. Bulla, T. A. Costi, and D. Vollhardt, Phys. Rev. B **64**, 045103 (2001).

[15] In Ref. 4 the algorithm used includes a spectral "smoothing" which consists on averaging the spectral weight within each energy interval and where the self-consistency is searched within this solution. In our case, instead, we do not average the spectral weight and the peaks obtained correspond to the finite size chain considered.

[16] G. Sangiovanni *et al.*, Phys. Rev. B **73**, 205121 (2006).

[17] M. J. Rozenberg, G. Kotliar, H. Kajueter, G. A. Thomas, D. H. Rapkine, J. M. Honig, and P. Metcalf, Phys. Rev. Lett. **75**, 105 (1995).

[18] J. M. Ziman, *Principles of the Theory of Solids*, 2nd ed. (Cambridge University Press, Cambridge, UK, 1972), p. 280.

[19] In a classical approximation, $DW = \frac{ne^2}{m}$ where n is the carrier density and m is its mass.

[20] W. Kohn, Phys. Rev. **133**, A171 (1964).

[21] G. Kotliar, S. Murthy, and M. J. Rozenberg, Phys. Rev. Lett. **89**, 046401 (2002).